

# Synthesis of Size-Controlled and Shaped Copper Nanoparticles

Derrick Mott, Jeffrey Galkowski, Lingyan Wang, Jin Luo, and Chuan-Jian Zhong\*

Department of Chemistry, State University of New York at Binghamton, Binghamton, New York 13902

Received December 4, 2006. In Final Form: February 21, 2007

The synthesis of stable, monodisperse, shaped copper nanoparticles has been difficult, partially because of copper's propensity for oxidation. This article reports the findings of an investigation of a synthetic route for the synthesis of size-controllable and potentially shape-controllable molecularly capped copper nanoparticles. The approach involved the manipulation of reaction temperature for the synthesis of copper nanoparticles in organic solvents in the presence of amine and acid capping agents. By manipulating the reaction temperature, this route has been demonstrated for the production of copper nanoparticles ranging from 5 to 25 nm. The size dependence of the melting temperature of copper nanoparticles, especially for surface melting, is believed to play an important role in interparticle coalescence, leading to size growth as the reaction temperature is increased. Control of the reaction temperature and capping molecules has also been demonstrated to produce copper nanoparticles with different shapes such as rods and cubes. The previously proposed combination of the selective formation of a seed precursor and a selective growth direction due to the preferential adsorption of capping agents on certain nanocrystal facets is believed to be responsible for shape formation by kinetically controlling the growth rates of crystal facets. The nanoparticles are characterized using TEM, XRD, and UV–visible techniques. A mechanistic consideration of the size control and shape formation is also discussed.

## Introduction

The ability to synthesize nanoparticles of different compositions with desired sizes and shapes is important in exploring their applications in catalysis, sensors, microelectronics, and many other areas of nanotechnology.<sup>1,2</sup> The nanoscale properties of copper and its alloys have found applications in catalysis (e.g., water–gas shift catalysts and gas detoxification catalysts<sup>3,4</sup>). The synthesis of copper nanoparticles with controllable sizes, shapes, and surface properties is vital to exploring copper-based catalysis.<sup>1,2</sup> Such abilities will also lead to an increased use of copper in many other areas of nanotechnology that are currently dominated by the use of gold, silver, and platinum nanoparticles. Although there are a number of approaches to synthesizing copper nanoparticles under specific conditions,<sup>5</sup> few methods have been established to control the size and shape effectively. Because of the propensity of surface oxidation of copper,<sup>6</sup> a key issue is whether copper nanoparticles can be produced with controllable sizes and shapes. To date, relatively limited attempts have succeeded in synthesizing copper nanoparticles with controllable sizes, shapes, and surface properties. In previous reports, copper nanoparticles have been synthesized using methods that include organic encapsulation in an aqueous phase,<sup>7</sup> the encapsulation of copper in a thiol capping agent,<sup>6</sup> and thermal decomposition.<sup>8</sup> The copper nanoparticles resulting from these methods had either limited size monodispersity or were susceptible to oxidation.<sup>5,6</sup>

The chemical reduction of copper ions in mixed reverse micelles (using an AOT surfactant in water/isooctane) was reported by Pileni and co-workers to produce copper nanocrystals with different shapes.<sup>9</sup> The nanoparticle shape was found to depend on the concentration of reducing agents, with spherical shapes formed in lower concentrations and other shapes such as pentagons, cubes, tetrahedra, and elongated forms in higher concentrations. The formation of certain initial seed shapes and the difference in the relative rates of growth on different crystal facets were proposed to explain the shape formation.<sup>9</sup> This is one of the first mechanisms proposed to explain shape formation on the nanoscale, which is quite intriguing. An understanding of how different synthetic conditions or control parameters are operative mechanistically in the formation of the nanoscale sizes and shapes is therefore elusive.

This report describes the findings of an investigation of the synthesis of copper nanoparticles with controlled sizes and potentially shapes by a combination of controlled reaction temperature and capping agents (Scheme 1). This route stems from previous work, including our own<sup>8,10,11</sup> demonstrating the synthesis of different alloy nanoparticles in organic solvents with molecular capping agents and elevated reaction temperature. It also takes advantage of the possible effect of particle sizes on the melting temperature of copper nanoparticles under the reaction conditions. This route not only yields copper nanoparticles of controllable sizes but also produces shaped nanoparticles, including rods and cubes. Such abilities are important for engineering the sizes and shapes of copper-based nanoparticles of different compositions for potential applications in catalysis and sensors.<sup>12</sup>

## Experimental Section

**Chemicals.** Copper(II) acetylacetonate ( $\text{Cu}(\text{acac})_2$ , 98%) was obtained from Lancaster. Oleic acid (99%) was obtained from

\* To whom correspondence should be addressed. E-mail: cjzhong@binghamton.edu.

(1) Hoover, N.; Auten, B.; Chandler, B. D. *J. Phys. Chem. B* **2006**, *110*, 8606.

(2) Niu, Y.; Crooks, R. *Chem. Mater.* **2003**, *15*, 3463.

(3) Ressler, T.; Kniep, B. L.; Kasatkin, I.; Schlögl, R. *Angew. Chem.* **2005**, *44*, 4704.

(4) (a) Vukojevic, S.; Trapp, O.; Grunwaldt, J.; Kiener, C.; Schth, F. *Angew. Chem., Int. Ed.* **2005**, *44*, 7978. (b) Barrabes, N.; Just, J.; Dafinov, A.; Medina, F.; Fierro, J. L. G.; Sueiras, J. E.; Salagre, P.; Cesteros, Y. *Appl. Catal. B* **2006**, *62*, 77.

(5) (a) Arul Dhas, N.; Paul Raj, C.; Gedanken, A. *Chem. Mater.* **1998**, *10*, 1446. (b) Zhu, H.; Zhang, C.; Yin, Y. *Nanotechnology* **2005**, *16*, 3079.

(6) Chen, S.; Sommers, J. M. *J. Phys. Chem. B* **2001**, *105*, 8816.

(7) Kim, Y. H.; Kang, Y. S.; Lee, W. J.; Jo, B. G.; Jeong, J. H. *Mol. Cryst. Liq. Cryst.* **2006**, *445*, 231.

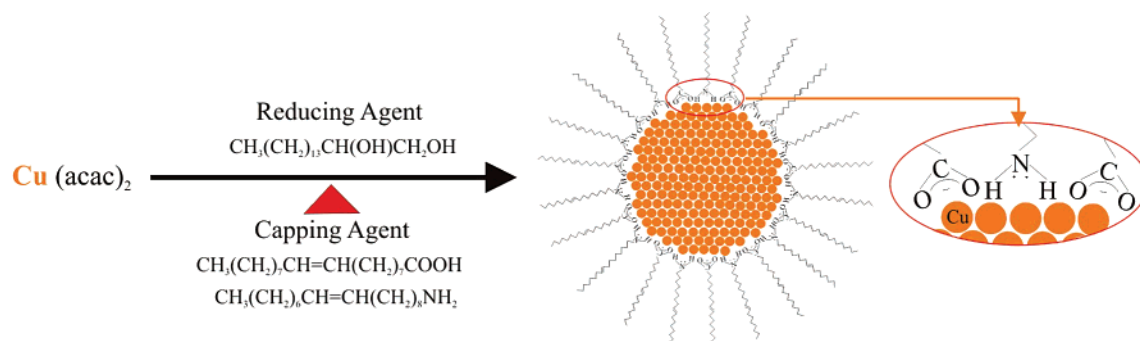
(8) (a) Sun, S.; Murray, C. B.; Weller, D.; Folks, L.; Moser, A. *Science* **2000**, *278*, 1989. (b) Fievet, F.; Lagier, J. P.; Figlarz, M. *MRS Bull.* **1989**, *14*, 29.

(9) Salzemann, C.; Lisiecki, I.; Urban, J.; Pileni, M.-P. *Langmuir* **2004**, *20*, 11772.

(10) Sun, S.; Fullerton, E. E.; Weller, D.; Murray, C. B. *Trans. Magn.* **2001**, *37*, 4.

(11) Luo, J.; Han, L.; Kariuki, N. N.; Wang, L.; Mott, D.; Zhong, C. J.; He, T. *Chem. Mater.* **2005**, *17*, 5282.

**Scheme 1. Schematic Illustration of the Synthesis of Copper Nanoparticles in the Presence of Capping Agents in Organic Solvent<sup>a</sup>**



<sup>a</sup> The reduction reaction occurs at elevated temperature.

Alfa Aesar. 1,2-Hexadecanediol (90%), octyl ether (99%), oleyl amine (70%), hexane, and other common solvents used were obtained from Aldrich.

**Synthesis.** The synthesis of copper nanoparticles in organic solution was achieved through the modification of a previous method that was reported for the synthesis of FePt nanoparticles<sup>8a</sup> and PtVFe nanoparticles.<sup>11</sup> In the modified synthesis, copper(II) acetylacetonate was added to octyl ether to create a 20 mM solution of copper(II). Then 1,2-hexadecanediol (a reducing agent)<sup>8b</sup> was added to the solution (60 mM). The solution was then cooled to room temperature to a temperature of 105 °C with stirring. The solution was held at 105 °C for 10 min, and then both oleic acid and oleyl amine capping agents were added to the solution to create 20 mM solutions of each. The solution was heated to higher temperatures, which was varied from 150 to 210 °C. Once at high temperature, the solution was left to react for 30 min. The solution was then cooled to room temperature. Finally, the reacted solution was mixed with ethanol, and the particles were allowed to precipitate overnight. The supernatant was removed, and the nanoparticle sediment was washed and dried using a stream of nitrogen gas. We note that we have not yet determined the synthetic yields, but a complete determination of the yields at different reaction temperatures is part of our ongoing work, which will be reported in the near future. The nanoparticles were suspended in hexane and were ready for analysis.

**Instrumentation and Measurements.** The nanoparticles were characterized using thermogravimetric analysis (TGA), UV–vis spectroscopy, transmission electron microscopy (TEM), and X-ray powder diffraction (XRD).

TGA analysis was performed on a Perkin-Elmer Pyris 1-TGA to determine the weight of the organic shell. Typical samples weighed ~4 mg and were heated in a platinum pan. Samples were heated in 20% O<sub>2</sub> at a rate of 10 °C/min.

UV–vis spectra were acquired with an HP 8453 spectrophotometer. A quartz cell with a path length of 1 cm was used, and spectra were collected over the range of 200–1100 nm.

TEM was performed on a Hitachi H-7000 electron microscope (100 kV). Copper nanoparticle samples were suspended in hexane solution and were drop cast onto a carbon-coated copper grid, followed by solvent evaporation in air at room temperature.

XRD data was collected on a Philips X<sup>3</sup>Pert diffractometer using Cu K $\alpha$  radiation ( $\lambda = 1.5418 \text{ \AA}$ ). The measurements were made in reflection geometry, and the  $2\theta$  diffraction (Bragg) angles were scanned at a step of 0.025°. Each data point was measured for at least 20 s, and several scans were taken of the sample.

## Results and Discussion

The reaction for the synthesis of copper nanoparticles of different sizes, as shown in Scheme 1, was accomplished by

varying the reaction temperature in the range of 150–190 °C. As the temperature of the reaction was raised, solutions with the resulting nanoparticles were found to become darker in color. The size evolution and shape formation, which are highly dependent on the reaction temperature, will be detailed in the next two subsections. As a general observation, the color evolution of the reaction solution under different temperatures was found to serve as an indication of particle size evolution. When the reaction temperature was held at 150 °C, a yellow solution was observed (Figure 1A). This color corresponded to small copper nanoparticles. As the reaction temperature was increased, the color of the solution with the as-synthesized copper nanoparticles showed a series of color changes ranging from light yellow to orange to dark brown to purple-brown depending on the reaction temperature. A brown solution was observed for particles synthesized at 180 °C (Figure 1B).

UV–vis spectra of the resulting nanoparticle solutions (Supporting Information) displayed a surface plasmon (SP) resonance band at ~600 nm, characteristic of copper nanoparticles. Copper nanoparticles synthesized by other methods were reported to display an SP band at ~570 nm.<sup>7,9</sup> The exact position of this band may shift depending on the individual particle properties including size, shape, solvent used, and capping agent employed. The spectrum for the as-synthesized small particles showed a rising feature at ~440 nm. For the solution of nanoparticles synthesized at 150 °C, a rising band at about 435 nm was apparent in the UV–vis spectrum. As the particles became larger, this band shifted to higher wavelength (up to ~600 nm). A strong SP band was observed at 591 nm for the formation of large copper nanoparticles synthesized at 200 °C.

TGA was used to assess the relative composition of the organic capping agents on the nanoparticles.<sup>11</sup> Figure 2 shows a representative TGA curve obtained for the 6-nm copper nanoparticles that were heated from 25 to 400 °C under oxygen. It is evident that the mass decrease due to the removal of the capping agents took place in the range of about 150 to 300 °C. At temperatures beyond about 400 °C, the increase in mass was due to the oxidation of the copper metal. The mass change can be translated to the ratio of capping molecules to copper particles. About 39% of the sample mass was due to the capping shell, leaving 61% of the mass to copper. For a 50/50 mixture of oleic acid/oleylamine capping molecules on a 6-nm copper nanoparticle, a spherical model calculation<sup>11</sup> yields a value of 24% for the oleic acid/oleylamine capping organic materials. The deviation of the experimental value from the theoretical value could be partially due to residual octyl ether in the sample.<sup>11</sup> A preliminary differential scanning calorimetry (DSC) experiment was also performed for the 6-nm copper nanoparticles in an attempt to estimate the approximate melting point (Supporting Information).

(12) (a) Zhong, C. J.; Luo, J.; Maye, M. M.; Han, L.; Kariuki, N. N. In *Nanotechnology in Catalysis*; Zhou, B., Hermans, S., Somorjai, G. A., Eds.; Kluwer Academic/Plenum Publishers: New York, 2004; Vol. 1, Chapter 11, pp 222–248. (b) Nanoparticles and Nanostructures in Sensors and Catalysis; *MRS Proceedings*; Zhong, C. J., Kotov, N. A., Daniell, W., Zamborini, F. P., Eds.; Warrendale, PA, 2006; Vol. 900E.

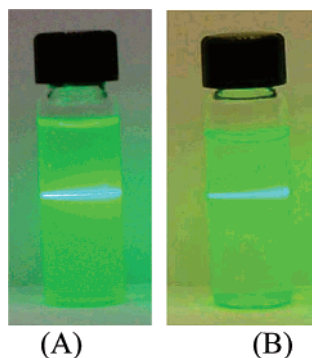


**Figure 1.** Photographs of solutions of Cu nanoparticles synthesized at (A) 150 and (B) 180 °C. A green laser beam was shone through the solutions, which produces the observed light scattering due to the presence of nanoparticles in the solutions.

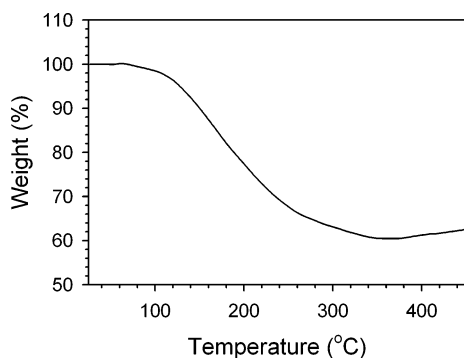


**Figure 2.** TGA curve for copper nanoparticles synthesized at 150 °C.

The resulting heating curve showed an endothermic peak beginning around 450 °C with a maximum near 550 °C, which is likely associated with the melting of the copper nanoparticles. However, a more detailed analysis is needed to substantiate this conclusion.

The nanoparticles synthesized under different conditions were also studied to determine their solubility and relative stability. Most of the copper nanoparticles were soluble in hexane. It was observed that the well-suspended nanoparticles remained in solution without precipitating for several weeks. The precipitated particles could also be easily resuspended. When additional oleyl amine or oleic acid was added to the nanoparticle solution, the solution was found to turn blue, suggesting the formation of copper(II) ions. This instability, although the exact origin is not clear, appears to reflect an equilibrium shift that promotes the oxidation of Cu(0) to form Cu(II) complexes with oleyl amine or oleic acid ligands.<sup>6</sup> To determine whether the synthesized copper particles were stable under ambient conditions ( $\sim 20$  °C), a small amount of the nanoparticle solution was placed in a vial and left open to the air for several weeks. There were no indications of changes in the solution color, including an unchanged SP band in the UV–vis spectra. TEM imaging of the samples after several weeks also showed that the as-synthesized nanoparticles were stable under ambient conditions. This stability is desired because the nanoparticles can be stored under ambient conditions for long periods of time before use. The next two subsections describe the morphological properties of the copper nanoparticles in terms of sizes and shapes.

**Copper Nanoparticles of Different Sizes.** The analysis of the copper nanoparticles showed an increasing trend in the average size with the reaction temperature. Figure 3 shows a representative set of TEM images for copper nanoparticles synthesized at three different temperatures. At 150 °C, the particles

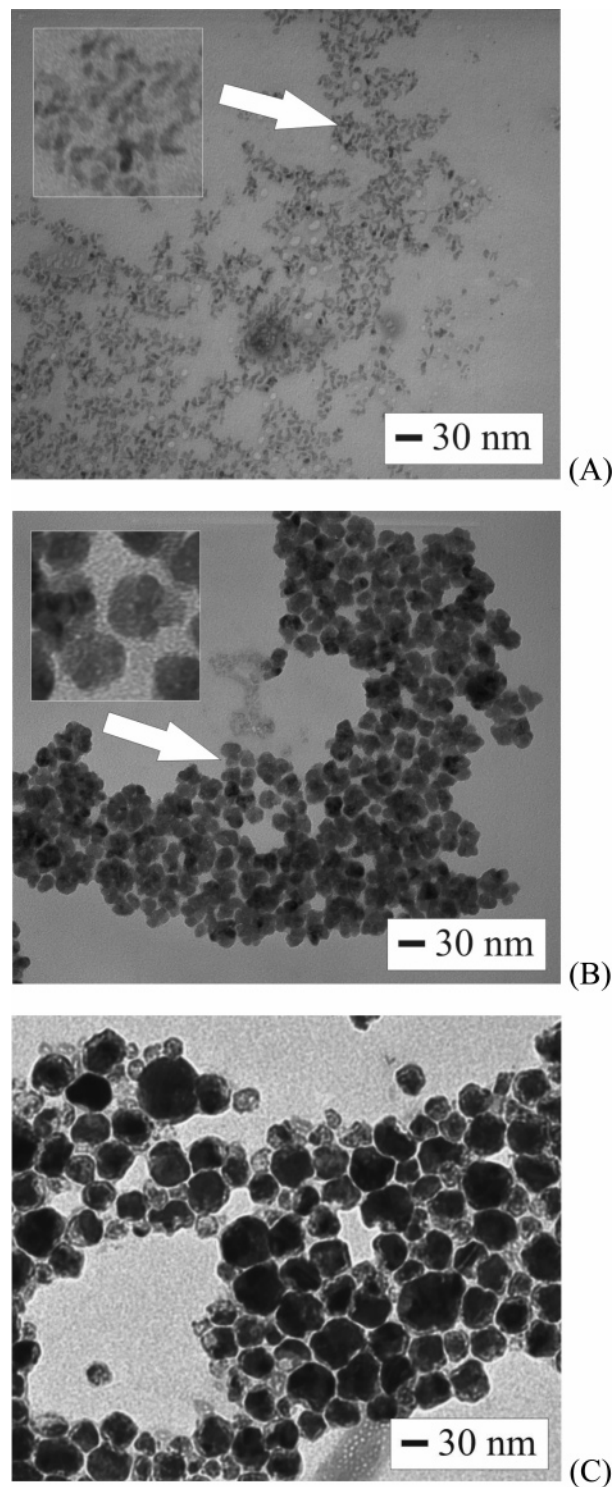


**Figure 3.** TEM images of Cu nanoparticles synthesized at (A) 150, (B) 160, and (C) 190 °C.

were small with flowerlike outlines (A). At 160 °C, the particles became larger and showed a tendency to cluster (B). As the temperature was increased to 190 °C, the particles became even larger, more spherical, and showed a better-defined interparticle separation (C).

The average sizes of the particles range from about 5 to 25 nm depending on the reaction temperature, with the standard deviation of the particle sizes ranging from  $\pm 1.8$  to  $\pm 6.5$  nm, respectively. The particles synthesized at temperatures below 190 °C were highly monodisperse, with standard deviations of less than 3.5 nm. When the synthesis temperature was raised

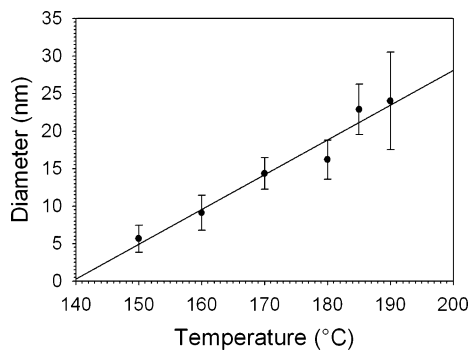


**Figure 4.** Plot of nanoparticle size vs synthesis temperature up to 190 °C. The line represents the linear regression of the data.

above 190 °C, the nanoparticles showed increased standard deviations (e.g.,  $24.0 \pm 6.5$  nm (190 °C)).

Figure 4 shows a plot of the average particle size versus the reaction temperature. The average size of the nanoparticles was found to increase approximately linearly with temperature. The linear regression of the data yields 0.46 nm/°C. This finding is significant, demonstrating the important role of reaction temperature in the control of particle size.

A close examination of some of the large particles seems to reveal subtle cluster features. This observation may hint at the possibility of coalescence of smaller particles, which provides some implications to the understanding of the mechanistic origin of the size dependence on temperature. It is known that the growth of nanoparticles is influenced by the strength of adsorption of the encapsulating ligands and the competition between the interparticle aggregation for the growth of particles and the molecular encapsulation for the stabilization of nanoparticles. For growth to occur, desorption of an encapsulating ligand on the particle must occur, allowing a metal atom or neighboring particle to gain access to the particle surface.<sup>13</sup> The adsorption of capping molecules on the copper nanoparticles is favored at lower temperatures, thus limiting the particle growth rate. However, as the temperature is increased, desorption of the capping ligand from the nanoparticle surface is favored, increasing the opportunities for interparticle coalescence. On the basis of the TGA data, desorption of the capping molecules from the nanoparticle surface likely occurs at  $\sim 150$  °C. Below  $\sim 150$  °C, there were no nanoparticles detected. Therefore, the nanoparticles synthesized at 150 °C acted as seed particles for the growth of larger particles at elevated reaction temperature. In addition to the theoretical basis for the decreased melting point of nanoscale copper particles, there are experimental studies indicating that nanoscale copper materials exhibit depressed melting points. For example, copper nanorods have recently been shown to exhibit a range of melting temperature as low as 350–550 °C.<sup>17</sup> A DSC study of gold nanoparticles coated by a silica shell concluded that for gold nanoparticles of 10 nm diameter melting occurs at a much more depressed temperature than for its bulk counterpart.<sup>18</sup>

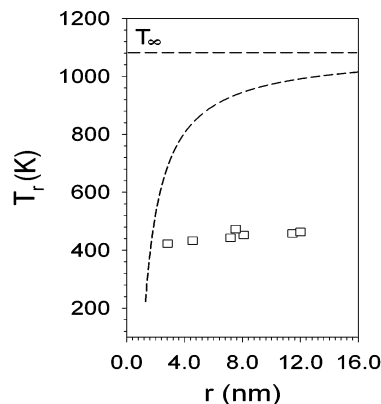


**Figure 5.** Theoretical modeling of the melting temperature of copper nanoparticles as a function of particle radius based on eq 1. The parameters used for the theoretical calculation were  $\rho_s = 8960$  and  $\rho_l = 8020$  kg/m<sup>3</sup>,  $L = 20\,500$  J/kg,<sup>15</sup> and  $\gamma_s = 1.29$  and  $\gamma_l = 1.11$  J/m<sup>2</sup>.<sup>16</sup> The actual temperatures used in the synthesis vs the particle size obtained are included as square symbols.

One of the important conditions for interparticle coalescence is surface melting. As demonstrated in our earlier work for the size evolution of gold nanoparticles at elevated temperatures, the decrease in the melting point for nanosized particles is an important factor for interparticle coalescence.<sup>13</sup> The decrease in the melting point with reduced particle size can be explained by the early thermodynamic model describing melting curves for fine metal particles,<sup>13a,14</sup> which relates the melting point of nanoparticles to that of its bulk metal by the equation

$$\frac{T_r - T_\infty}{T_\infty} = -\frac{4}{\rho_s L 2r} \left[ \gamma_s - \gamma_l \left( \frac{\rho_s}{\rho_l} \right)^{2/3} \right] \quad (1)$$

where  $T_r$  and  $T_\infty$  are the melting temperatures of the particle and the bulk solid, respectively,  $r$  is the radius of the particle,  $\rho_s$  and  $\rho_l$  are the densities of the solid and the liquid, respectively,  $\gamma_s$  and  $\gamma_l$  are the surface energies of the solid and the liquid, respectively, and  $L$  is the heat of fusion.<sup>13a</sup> The theoretical model predicts a decrease in the melting point with decreasing size for copper particles (Figure 5).

The implication of this trend is that smaller particles have a tendency to melt or partially melt at the reaction temperature. The actual temperatures used in the synthesis were much smaller than the theoretical temperatures for the melting curve. For the smallest particle size, the reaction temperature was closer to that in the theoretical curve, with a difference of  $\sim 100$  °C. On the basis of this observation, it is likely that the surface melting of the nanoparticles is responsible for the interparticle coalescence, leading to size growth as the reaction temperature is increased. This temperature-controlled size growth is to our knowledge the first example discussing the important role of surface melting in the synthesis of copper nanoparticles. Although the lowering of the melting point is inversely proportional to the particle size ( $r$ ), the surface melting temperature could be even lower (e.g.,  $\sim 140$  °C for 2-nm Au).<sup>13</sup> The relative change in temperature is also related to the capping-dominated surface tension. Under such surface melting and surface tension effects, the driving force for the coalescence of two surface-melt Cu particles is the reduction in free energy through a reduction in surface area (e.g., increase in size).

**Formation of Shaped Cu Nanoparticles.** By further modifying the synthesis procedure, copper nanoparticles with significantly increased populations of shaped particles were produced. It was found that copper nanoparticles with different shapes

(13) (a) Maye, M. M.; Zheng, W. X.; Leibowitz, F. L.; Ly, N. K.; Zhong, C. *J. Langmuir* **2000**, *16*, 490. (b) Schadt, M. J.; Cheung, W.; Luo, J.; Zhong, C. *J. Chem. Mater.* **2006**, *18*, 5147.

(14) Buffat, Ph.; Borel, J. P. *Phys. Rev. A* **1976**, *13*, 2287.

(15) Lisiecki, I.; Sack-Kongehl, H.; Weiss, K.; Urban, J.; Pileni, M.-P. *Langmuir* **2000**, *16*, 8802.

(16) Matsumoto, T.; Fujii, H.; Ueda, T.; Kamai, M.; Nogi, K. *Meas. Sci. Technol.* **2005**, *16*, 432.

(17) Karabacak, T.; DeLuca, J. S.; Wang, P.-I.; Ten Eyck, G. A.; Ye, D.; Wang, G.-C.; Lu, T.-M. *J. Appl. Phys.* **2006**, *99*, 064394.

(18) Dick, K.; Dhanasekaran, T.; Zhang, Z.; Meisel, D. *J. Am. Chem. Soc.* **2002**, *124*, 2312.

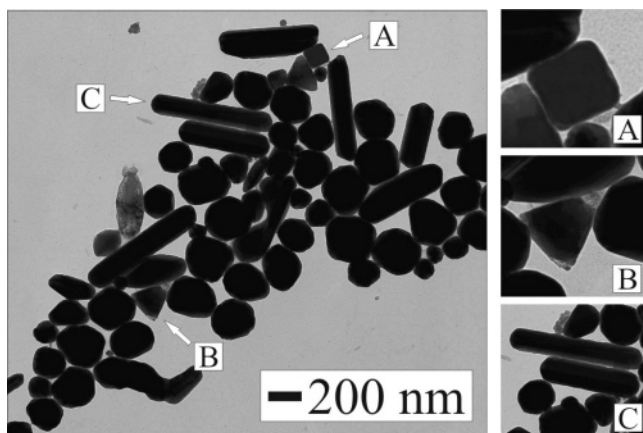


**Figure 6.** TEM image of copper nanoparticles synthesized at 210 °C. The enlarged views show (A) cube-, (B) tetrahedral-, and (C) rod-shaped particles.

began to form at temperatures above 190 °C. Figure 6 shows a representative TEM image of the as-synthesized particles derived from the reaction temperature of 210 °C and careful control of the initial heating rate in the presence of the capping agents. Copper nanoparticles shaped as cubes, rods, and tetrahedrons are evident, in addition to a certain percentage of spherically shaped particles. Shape formation began at 190 °C but was not prominent until 200 °C, for which shapes such as rods and cubes became common among the particles. In all of the samples that formed shapes, rods were the most common shape, demonstrating that the formation of copper nanoparticles at high temperature favors the formation of rods. As indicated by the enlarged views, the cubes, rods, and tetrahedrons have well-defined shapes. The cube-shaped particles are 200 nm in size. The rod-shaped particles are around 700 nm in length and about 100 nm in width, with an aspect ratio as high as  $\sim 7$ . It is important to note that these shaped particles do not show any hint of the possibility of coalescence of smaller particles as observed for the spherical particles described earlier, thus ruling out the simple coalescence mechanism for shape formation. The observation of these shapes is remarkable considering the relatively small change in the synthetic temperature that was required to initiate their formation.

There is a remarkable resemblance between the shapes of the nanoparticles synthesized using our method and those reported by Pileni and co-workers.<sup>9</sup> In the reported work,<sup>9</sup> Cu(AOT)<sub>2</sub> and NaAOT were solubilized in isooctane with a controlled percentage of water. This forms reverse micelles in which Cu(AOT)<sub>2</sub> is reduced by various concentrations of hydrazine. On the basis of the observation of copper particles with spheres, rods, cubes, and tetrahedral shapes, the mechanism proposed for the formation of these shaped copper nanocrystals involves (i) the initial formation of a decahedral, cubo-octahedral, or tetrahedral precursor and (ii) the preferential adsorption of capping agents on the nanocrystal facets in order to control the growth rates of the crystal facets kinetically.<sup>9</sup> For the growth process of copper nanoparticles under our synthesis conditions, we used two capping agents. It is possible that one of the capping agents favors adsorption to one of the nanocrystal facets (e.g., 111, 110, or 100) while allowing the other faces to grow more quickly.

To confirm the crystalline properties of the nanocrystals, the as-synthesized nanoparticles were examined using XRD. As shown in Figure 7, the nanoparticles display high crystallinity. The diffraction peaks at  $2\theta = 43.5, 50.6,$  and  $74.3$  can be indexed as the [111], [200], and [220] planes of copper with cubic symmetry. The pattern is very clean, with no indication of

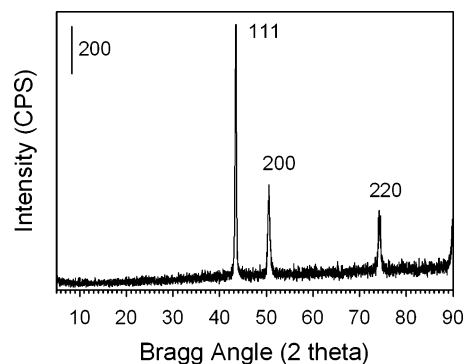
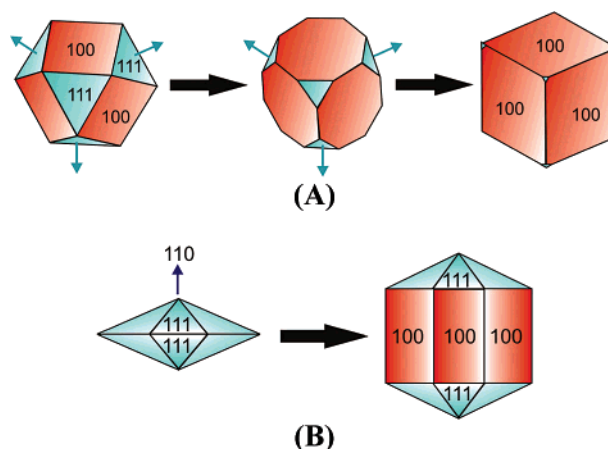


**Figure 7.** XRD pattern of the copper nanoparticles synthesized at 210 °C.

**Scheme 2. Schematic Illustration of the Growth Mechanism for the Formation of (A) Cube-Shaped Particles from a Cubo-octahedron Seed and (B) Rod-Shaped Particles from a Decahedral Seed**



impurities such as copper oxides (CuO, Cu<sub>2</sub>O). The results are quite consistent with those reported by others for Cu nanoparticles or nanorods prepared by different methods.<sup>19</sup>

The mechanism proposed previously by Pileni and co-workers<sup>9</sup> for shape formation in reverse micelle synthesis, as illustrated in Scheme 2, seems to be applicable to the synthesis of shaped nanoparticles using the method discussed in this article. The observation of several shapes in the synthesized particles is indicative of the formation of several different seed precursors. These seeds then grow, regulated by the capping agents, along different directions of the nanocrystal into particles with various shapes. As shown in Scheme 2A, a cubo-octahedron seed particle serves as a precursor. If this seed were to grow equally in all directions, then it would enlarge into a roughly spherically shaped particle; however, there is a difference in the rate of growth along its faces. The difference in the speed of growth is caused by the varying surface free energy and thus the varying strength of capping agent adsorption. Because the capping agent adsorbs more strongly to the 100 face of the cubo-octahedron nanocrystal, the 111 faces grow at a faster rate than the 100 faces. This kinetic difference leads to the formation of a cube-shaped particle instead of a sphere. Similarly, for a decahedral seed particle, illustrated in Scheme 2B, the 111 faces grow at a faster rate than the 100 faces, causing the kinetically favored growth of the 111 faces into an elongated rod-shaped particle. It is important to note that the final size of the particles is not solely dependent on the seed shape but is also dependent on the total growth time of the particle.

(19) Panigrahi, S.; Kundu, S.; Ghosh, S. K.; Nath, S.; Praharaj, S.; Basu, S.; Pal, T. *Polyhedron* **2006**, *25*, 1263.

A key question is what synthesis parameters are necessary to achieve precise control of the formation of the precursor seed particles and the relative adsorption of the two capping agents on the nanocrystal surfaces. Preliminary experiments have indicated that the manipulation of the reaction temperature and the relative ratio of the two capping agents could lead to variations of the differently shaped copper nanoparticles. Therefore, establishing the correlation between the nanocrystal shape and these two sets of parameters will allow the selective synthesis of specifically shaped copper nanoparticles.

### Conclusions

A new route for the synthesis of copper nanoparticles in organic suspensions has been demonstrated. The size, shape, and stability of the nanoparticles are highly dependent on the reaction temperature, with the particle size increasing with the reaction temperature in an approximately linear manner. On the basis of a theoretical consideration of the size dependence of the melting temperature of copper nanoparticles, the surface melting of the nanoparticles is believed to be responsible for the interparticle coalescence, leading to size growth as the reaction temperature is increased. This temperature-controlled size growth is to our knowledge the first example discussing the important role of

surface melting in the synthesis of copper nanoparticles. The feasibility of synthesizing copper nanoparticles with well-defined shapes such as rods and cubes has also been demonstrated. Mechanistically, shape formation is linked to a combination of the initial formation of a seed precursor and the preferential adsorption of capping agents on selected nanocrystal facets in order to control the growth rates of certain crystal facets kinetically. More experiments are underway to determine the detailed correlation between the particle size or shape and the control parameters such as reaction temperature and capping agents, which will have important implications in the engineering of metal nanoparticles as building blocks for applications in many areas of nanotechnology, including catalysis and chemical sensing.

**Acknowledgment.** Financial support of this work from the National Science Foundation (CHE 0349040) is gratefully acknowledged.

**Supporting Information Available:** UV-vis and DSC data. This material is available free of charge via the Internet at <http://pubs.acs.org>.

LA0635092